communications materials

Article

https://doi.org/10.1038/s43246-024-00462-y

Durable plasma-mediated zwitterionic grafting on polymeric surfaces for implantable medical devices

Matthew Crago[1], Richard Tan[2], Juichien Hung[2], Steven G. Wise[2], Behnam Akhavan[3,4,5,6], Marcela Bilek[3,4], Fariba Dehghani[1], Sepehr Talebian[1] & Sina Naficy[1]

Adverse body reactions to blood-contacting medical devices endanger patient safety and impair device functionality, with events invariably linked to nonspecific protein adsorption due to suboptimal material biocompatibility. To improve the safety and durability of such devices, herein we propose a strategy for introducing stable zwitterionic grafts onto polymeric surfaces via plasma functionalization. The resulting zwitterion-grafted substrates exhibit long-lasting superhydrophilicity, enabling antifouling and anti-thrombogenic properties. We demonstrate the successful modification of the surface elemental composition, morphology, and hydrophilicity, while retaining the underlying mechanical properties of the polymeric substrate. Furthermore, we optimise the fabrication process to ensure long-lasting modifications at least three months after fabrication. This strategy decreases fibrinogen adsorption by approximately 9-fold, and thrombosis by almost 75% when applied to a commercial polyurethane. Moreover, this process is universally applicable to a wide range of polymeric materials, even those with stable chemistry such as polytetrafluoroethylene.

Blood-contacting polymeric medical devices remain susceptible to adverse biological responses during clinical use, compromising patient health and limiting device durability[1,2]. This includes events such as thrombosis, inflammation, foreign body reaction, calcification, or infection at their interface with biological systems[1–4]. In particular, thrombosis is an established challenge in many blood-contacting devices, such as central venous catheters (CVCs), mechanical heart valve replacements, vascular stents, ventricular assist devices, and extracorporeal membrane oxygenation circuits[1]. For example, almost 30% of CVC placements may result in symptomatic venous thromboembolisms[1], with up to 80% of paediatric deep vein thrombosis (DVT) cases and 70% of adult upper extremity DVT attributable to a CVC[3,5]. Similarly, mechanical heart valve replacements are notoriously susceptible to thrombosis, with patients requiring indefinite pharmaceutical anticoagulation after implantation[6,7]. Accordingly, the development of new bioinert polymers, or devising methods to reduce adverse body reactions in existing polymeric systems, are integral to improving the safety and durability of blood-contacting devices.

Many biological responses are fundamentally initiated by the non-specific adsorption of blood proteins onto a polymer surface, herein termed biofouling, which occurs within seconds of contact with blood; for thrombosis, this is predominated by proteins such as fibrinogen, Factor XII, and von Willebrand's factor[2,8]. For example, adsorbed fibrinogen proteins develop into extensive fibrous networks that dominate blood clots and provide anchoring sites for circulating platelets[1,9]. To this end, imbuing polymers with antifouling properties offers a promising method for enhancing hemocompatibility[10]. Elastomers (e.g., polyurethanes, silicone) are commonly employed in the production of blood-contacting polymeric medical devices due to their mechanical resemblance to soft biological tissues. However, such polymers commonly possess suboptimal biocompatibility, which may be addressed by modifying the chemistry of the polymer backbone. For instance, polyurethanes have been modified to incorporate siloxane segments (i.e., siloxane-based polyurethanes) in order to improve hemocompatibility and biostability[7,11]. Nonetheless, bulk modifications may compromise polymer mechanics; for example, the introduction of siloxane components reduces the toughness of the polyurethane system.

[1]School of Chemical and Biomolecular Engineering, The University of Sydney, Sydney, NSW 2006, Australia. [2]School of Medical Sciences, Faculty of Health and Medicine, Charles Perkins Centre, The University of Sydney, Sydney, NSW 2006, Australia. [3]School of Biomedical Engineering, The University of Sydney, Sydney, NSW 2006, Australia. [4]School of Physics, The University of Sydney, Sydney, NSW 2006, Australia. [5]School of Engineering, University of Newcastle, Callaghan, NSW 2308, Australia. [6]Hunter Medical Research Institute (HMRI), Precision Medicine, New Lambton Heights, NSW, Australia.
e-mail: sina.naficy@sydney.edu.au

Fundamentally, the underlying chemistries that achieve optimal biocompatibility and optimal durability are not necessarily compatible.

A different approach is to modify the surface chemistry of the polymer (i.e., at the interface of the material with its environment) to alter the interaction between the device surface and its biological surroundings without affecting the device's bulk mechanics. This may be achieved by immobilising bioactive moieties that actively target pathways responsible for adverse biological responses[12]. For example, heparin modifications are well-documented owing to heparin's augmentation of antithrombotic feedback loops in the coagulation cascade[13]. Alternatively, the surface may be grafted with so-called passive modifications, which mitigate biofouling by altogether avoiding interactions between the substrate and the environment[12]; that is, by minimising the thermodynamic and kinetic incentives for protein adsorption and/or cellular adhesion. In general, passive antifouling surfaces can be either hydrophilic or hydrophobic. On hydrophilic surfaces, a tightly bound water layer is formed due to hydrogen and/or electrostatic bonds, establishing a physical and free energy barrier that prevents biofouling[10,14]. On the other hand, the low surface energy of superhydrophobic materials deters biofouling[15], although the denaturing of proteins that do adsorb can also impact platelet adhesion[16]. Accordingly, some prominent chemistries utilised to prevent protein adsorption include (a) superhydrophobic materials, such as polytetrafluoroethylene or tethered liquid perfluorocarbons[17], (b) hydrophilic materials based on hydrogen bonding, such as poly(ethylene glycol) or poly(hydroxyethyl methacrylate)[18], and (c) superhydrophilic materials based on electrostatic interactions, such as zwitterions[12,19,20].

Zwitterionic chemistries are one of the more promising candidates for antifouling surface modifications as they avoid entropic and energetic incentives for protein adsorption while permitting greater hydration than hydrophilic surfaces that rely on hydrogen bonding[14,21]. Zwitterions contain positively and negatively charged groups, which facilitate strong electrostatic interactions with water molecule dipoles[21,22]. Moreover, the internally balanced number of anions and cations results in overall electrical neutrality, which permits the tight association of water molecules held in a structurally similar state to molecules in bulk water. This removes the entropic incentive for water to dissociate in the event of protein encroachment, thus maintaining an energetically stable hydration barrier that imbues antifouling properties to the underlying substrate[14]. Biologically, zwitterions constitute the hydrophilic phospholipid heads of mammalian cell membranes, which crucially regulate interactions between cells and the extracellular environment[14,23]. Correspondingly, synthetic zwitterionic surface modifications have been shown to reduce substrate susceptibility to a range of biological events, such as thrombosis[24–26], fibrosis[27,28], calcification[29,30], and infection[24,25,31]. Notably, substantial work by Ratner et al. at the University of Washington demonstrated the ability of zwitterionic surfaces to resist protein adsorption and platelet adhesion[32], slow coagulation processes[32], and limit the foreign body reaction[33]. Moreover, this group recently proposed a strategy to graft zwitterionic copolymers onto medical-grade polymers such as poly(vinyl chloride) via benzophenone chemical linkers[34]. In fact, most zwitterion grafting processes require chemical linkers such as benzophenone[34], dopamine[35–38], or azide[24] moieties.

Alternatively, linker-free approaches may facilitate improved scalability, efficiency, and versatility. One outstanding linker-free strategy involves the functionalization of a polymer substrate with plasma (i.e., ionised gas), providing surface-anchored reactive sites that can participate in zwitterion grafting[39]. Recently, plasma functionalisation has been used to graft zwitterions onto poly(vinylidene fluoride)[40,41] and poly(ethylene)[42–44] surfaces, with these studies collectively demonstrating low fouling against a range of proteins (such as fibrinogen[40], bovine serum albumin[41,42], and lysozyme[41]), resistance to platelet adhesion and activation[40], and low microbial adhesion and biofilm formation[41,43,44]. A particularly robust plasma functionalization platform is plasma immersion ion implantation (PIII), which involves the bombardment of ions into the material surface to generate a reservoir of surface-embedded radicals, which can then be used to anchor desired moieties in a linker-free manner[39,45].

Herein, we hypothesise that PIII technologies can be harnessed as an efficient and versatile approach to graft zwitterions onto polymeric substrates without requiring chemical initiators. Initially, sulfobetaine methacrylate (SBMA) was used as a model zwitterionic monomer due to its well-documented utility as a biocompatible surface modification[24,25,27,28,46], and a commercially available, medical-grade, carbonate-based polyurethane (PU) was used as a model polymer (Fig. 1). The ability of this process to forgo external initiators was explored by first employing an initiator-aided approach, and then an initiator-free approach (Fig. 1a). The fabrication of zwitterion-grafted polyurethanes (ZG-PUs) was assessed by evaluating material hydrophilicity, surface chemistry, morphology, and mechanical properties. Importantly, the stability of the grafted zwitterion layer was carefully assessed, with extensive optimisation studies performed to ensure durable ZG-PU materials with long-lasting functional utility. Furthermore, the antifouling and anti-thrombogenic nature of the resulting ZG-PU materials were assessed via preliminary in vitro assays. Finally, the versatility of the process was explored by implementing various polymeric substrates and zwitterionic modifications.

Results and discussion

Fabrication and characterisation of zwitterion-grafted polyurethanes

The surface of a commercial polyurethane was functionalized via PIII, followed by immersion in SBMA solution containing ammonium persulfate as an external radical initiator (Fig. 1), resulting in the successful fabrication of a zwitterion-grafted polyurethane, as determined by morphological and elemental analyses (Fig. 2). When visualised with scanning electron microscopy (SEM), the pristine commercial polyurethane (PU) and a control polyurethane (C-PU, immersed in zwitterion solution without PIII functionalization) exhibited uniform, featureless surfaces (Fig. 2a, b, respectively). PIII-functionalized polyurethanes without zwitterion grafting (PIII-PU) exhibited a similar uniform morphology but with extensive cracks (white arrows) (Fig. 2c). The cracks can be the result of surficial stress caused by the storage of PIII-PU in air. Oxygen can readily react with the high-energy species on the surface of the PIII-PU samples, leading to the formation of such cracks. In contrast, the zwitterion-grafted polyurethane (ZG-PU) possessed a sprawling wave-like morphology (Fig. 2d). These observations were corroborated by atomic force microscopy, wherein C-PU surfaces were flat and rough (Fig. 2e), while ZG-PU surfaces were wavy and smooth (Fig. 2f and Supplementary Fig. 1). ZG-PU morphology may be caused by the formation of a swollen hydrophilic layer during zwitterion grafting, which subsequently wrinkled upon drying; this morphology has previously been observed in other swollen hydrophilic networks such as hydrogels[47,48]. Additionally, a limitation of the free-radical polymerisation mechanism is the lack of control over the polydispersity index and chain length, with this variability potentially contributing to this morphology. The discrepancies in the length of polymer chains can lead to the observable morphological features at this scale because small changes in size can compound over time as additional polymer chains attach to the underlying layers. Additionally, the conformation of grafted polymer chains on the surface can impact the overall morphology of the coating. Polymer chains attached to the surface conform into mushroom-like or extended chains—depending on the surface coverage and thermodynamics of the system—with chains placed next to one another. As the zwitterionic grafting progresses over time, the gaps between the adjacent polymer chains appear as valleys, with these valley-peak features magnifying as the thickness grows with grafting. The processes involved in the fabrication of these four groups are summarised in Table 1.

The surface chemistry of ZG-PU, PIII-PU, C-PU, and PU was analysed via X-ray photoelectron spectroscopy (XPS). Sulphur and nitrogen were used as markers for zwitterion grafting due to their presence in, respectively, the sulfonate anion and quaternary ammonium cation of SBMA (Fig. 1a). Both nitrogen (Fig. 2h) and sulphur (Fig. 2i) content was greatest in ZG-PU, with analysis of the survey spectra (Fig. 2g) indicating a nitrogen atomic

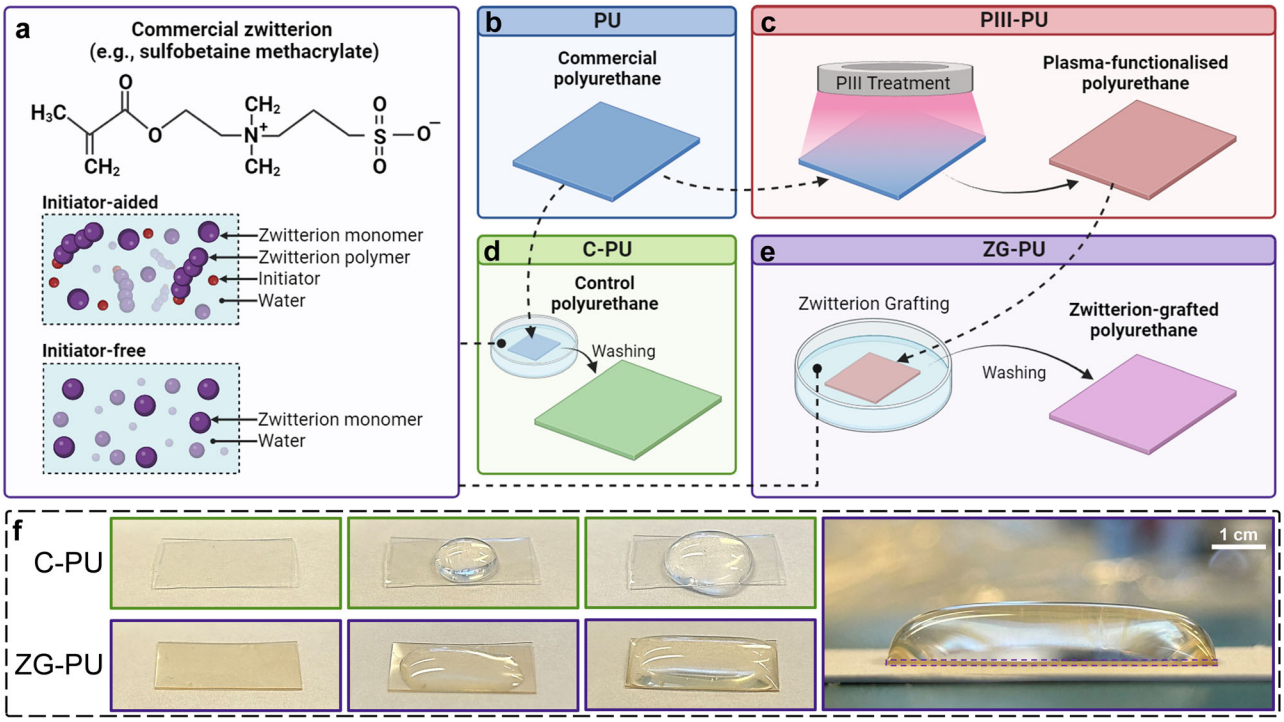

Fig. 1 | Fabrication of zwitterion-grafted polyurethanes via plasma immersion ion implantation (PIII). a Chemical structure of sulfobetaine methacrylate, a model zwitterion, and solutions used for initiator-aided and initiator-free strategies. Note the positively charged quaternary ammonium cation and the negatively charged sulfonate anion. **b** A commercial carbonate-based polyurethane was used as the model substrate, which was **c** plasma-treated using PIII to functionalise the surface. Both the commercial polyurethane and PIII-functionalized polyurethanes were then immersed in zwitterion solution to fabricate the **d** control polyurethane and the **e** final zwitterion-grafted polyurethane. **f** Macroscopically, ZG-PU materials exhibited a much more hydrophilic surface than C-PU (and PU), with water spreading over the surface rather than beading (adding water from left to right).

percentage of 4.89 ± 0.09% and a sulphur atomic percentage of 3.86 ± 0.02%. In comparison, nitrogen percentage was 1.02 ± 1.02%, 1.89 ± 0.24%, and 1.04 ± 0.35% for PU, C-PU and PIII-PU, respectively, and no sulphur was automatically identified in any group (Table 2). Deconvolution of the N1s spectra unveiled a distinct peak profile for ZG-PU; whereas the strongest peak for PU, C-PU and PIII-PU was around 400 eV (which was attributed to secondary amines in urethane linkages), ZG-PU exhibited a much stronger peak at 402 eV, which was consequently attributed to the quaternary ammonium cation of the SBMA molecule (Fig. 2j). Similar deconvolution of the S2p spectra demonstrated distinct $S2p_{1/2}$ and $S2p_{3/2}$ orbitals in ZG-PU, while the lack of this profile in all other groups suggests either trivial sulphur presence, or that these minimal measurements were a product of noise. Quantitative comparisons between groups were achieved by normalising the S2p sulphur and N1s nitrogen content of each material against their respective C1s carbon-carbon peaks (Table 2). The N/(C-C) and S/(C-C) ratios of ZG-PU were 0.22 ± 0.02 and 0.26 ± 0.02, respectively, whereas both ratios were below 0.04 for all other groups. Thus, these findings demonstrate the presence of SBMA on the polyurethane surface in ZG-PU, indicating the successful fabrication of a zwitterion-grafted polyurethane achieved via substrate functionalization with PIII.

Using water contact angle as a measure of hydrophilicity, ZG-PU was much more hydrophilic than PU and C-PU (Fig. 3a). The hydrophobicity of PU (water contact angle of 83.85 ± 2.75°) was remarkably altered by zwitterion grafting, with ZG-PU possessing near-superhydrophilic properties (12.98 ± 1.43°) (Fig. 3b); superhydrophilicity is defined as water contact angles of less than 10° and is associated with increased resistance to biofouling[49]. Importantly, this water contact angle is lower than that of similar materials fabricated via other recent processes[24,35,37], indicating an extremely hydrophilic surface chemistry. For example, water contact angles for dopamine-mediated zwitterionic grafts were around 23°[35,37], while azide-mediated grafts were around 15°[24]. In comparison, C-PU remained hydrophobic, with a water contact angle of 85.75 ± 3.35°. While the lack of sulphur in the XPS survey analysis of C-PU indicated no zwitterion presence, any trivial presence of zwitterion on C-PU, as suggested by the higher resolution S2p spectra (Fig. 2I), was inconsequential in modifying the surface chemistry. Taken together, these highlight the requirement of PIII functionalization in facilitating zwitterionic grafting. While PIII-PU was also significantly more hydrophilic than PU (45.83 ± 1.59°), it remained significantly less hydrophilic than ZG-PU (Fig. 3b), indicating that the very low hydrophilicity of ZG-PU could be ascribed to the zwitterion graft rather than PIII treatment alone. This distinction is important due to the well-established use of plasma treatment to generate hydrophilic surfaces[50,51]; in fact, the hydrophilicity of PIII-functionalized substrates may have actively improved grafting efficiency by favouring interactions between the surface and the SBMA-water solution.

The intrinsic stability of the zwitterion graft under cyclic stresses was assessed by subjecting ZG-PU to extensive flexural deformation under hydrated conditions. ZG-PU hydrophilicity did not change after 3000 flexural cycles, endorsing a strong interface between the zwitterion and PU components (Fig. 3c). Had the zwitterion graft been physically attached to the surface, it would have been delaminated from the substrate during the extended bending cycles. Furthermore, mechanical analysis was performed to determine whether the grafting process affected the bulk polymer; this was crucial in determining whether the cracks developed during PIII treatment affected the structural integrity of the material. Tensile and flexural properties were analysed via uniaxial tensile testing and cantilever flexural testing, respectively. Both the Young's modulus (Fig. 3d) and flexural rigidity (Fig. 3e) of ZG-PU were not significantly different to PU, C-PU, or PIII-PU, demonstrating that the grafting process transformed the surface without affecting bulk mechanical properties. The decoupling of surface properties from bulk mechanical properties is an important feature of this strategy as it

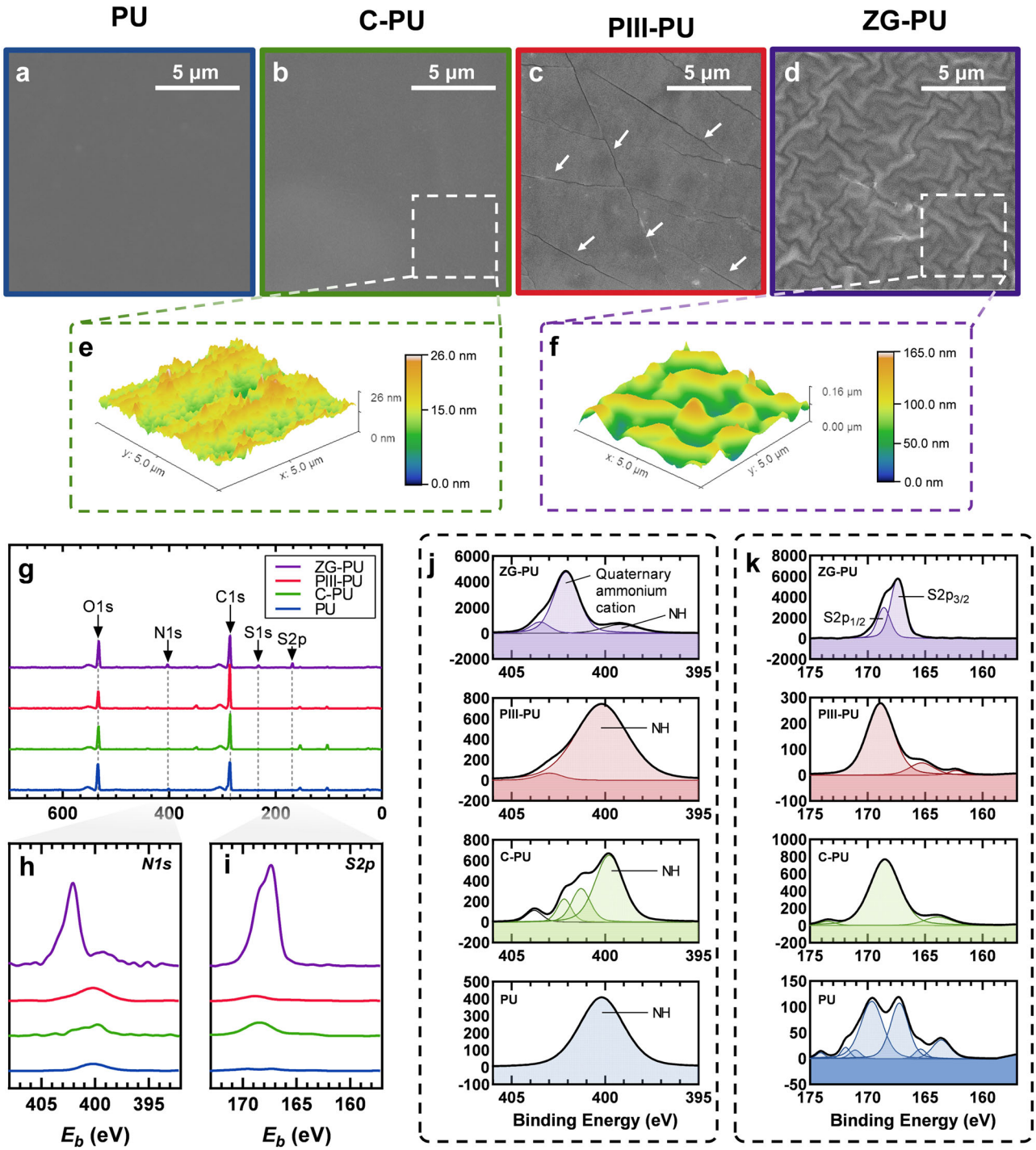

Fig. 2 | Morphology and elemental characterisations of zwitterion-grafted polyurethanes and controls using SEM, AFM, and XPS. a–f Morphological analysis. The surface morphology of **a** PU, **b** C-PU, **c** PIII-PU, and **d** ZG-PU was imaged using SEM, demonstrating a distinct morphology formed due to PIII-mediated zwitterion grafting. These observations were validated by AFM via 3D reconstruction of the surface morphologies of **e** C-PU and **f** ZG-PU. **g–k** Elemental analysis. **g** XPS survey spectra for all groups, with peaks at O1s, N1s, C1s, S1s and S2p used to calculate elemental compositions. **h** Detailed analysis of the N1s spectrum demonstrated a significant and shifted peak for ZG-PU, while **i** detailed analysis of the S2p spectra also demonstrated a significant peak for ZG-PU. Deconvolution of the **j** N1s and **k** S2p spectra further indicated the presence of SBMA in ZG-PU by the identification of an N1s peak associated with the SBMA quaternary ammonium cation, and distinct orbital splitting in the S2p peak.

increases the degree of freedom in selecting materials for the fabrication of medical devices.

This process was fundamentally facilitated by the ability of PIII technologies to generate radical-functionalized substrates that allow the immobilisation of zwitterionic moieties at the surface. During PIII treatment, energetic bombardment by nitrogen ions generates long-lived reactive radicals that migrate to the surface over time through thermally activated processes[39,52,53]. Upon immersion in zwitterion solution, such surface-embedded radicals facilitate covalent interactions between the SBMA moieties and the PU surface, resulting in ZG-PU. Importantly, at this point the zwitterion solution contained external chemical initiators (i.e., initiator-aided solution, Fig. 1a). In the presence of an initiator,

Table 1 | Summary of material groups

Material	Abbreviation	PIII Functionalization	Zwitterion grafting
Zwitterion-grafted polyurethane	ZG-PU	+	+
Plasma-functionalized polyurethane	PIII-PU	+	-
Control polyurethane	C-PU	-	+
Commercial (pristine) polyurethane	PU	-	-

Table 2 | XPS analysis of PU, C-PU, PIII-PU, and ZG-PU

Material	Elemental Composition (atomic percentage %)						C1s	N1s		S2p	
	C	O	N	S	Si	Ca	C-C	N	N/(C-C)	S	S/(C-C)
PU	69.01	25.46	1.02	0.00	4.52	0.00	70,088.44	3954.99	0.02	521.24	0.01
±	0.34	1.20	1.02	0.00	0.51	0.00	9264.47	2607.72	0.01	100.70	0.00
C-PU	69.69	22.44	1.89	0.00	5.61	0.36	37,576.23	1343.98	0.04	1165.74	0.02
±	1.45	1.66	0.24	0.00	1.53	0.36	17,442.74	564.97	0.01	801.50	0.01
PIII-PU	79.10	14.38	1.04	0.00	3.83	1.64	111,514.27	2981.81	0.03	904.43	0.01
±	6.37	4.79	0.35	0.00	1.28	0.55	37,171.42	993.94	0.00	301.48	0.00
ZG-PU	65.77	23.07	4.89	3.86	1.89	0.53	57,031.45	12,262.04	0.22	14,835.17	0.26
±	0.04	0.18	0.09	0.02	0.20	0.03	6477.45	171.26	0.02	646.71	0.02

The elemental composition (in atomic percentage) of each material was calculated from the survey spectra, and N/(C-C) and S/(C-C) ratios were derived from the C1s, N1s and S2p spectra.

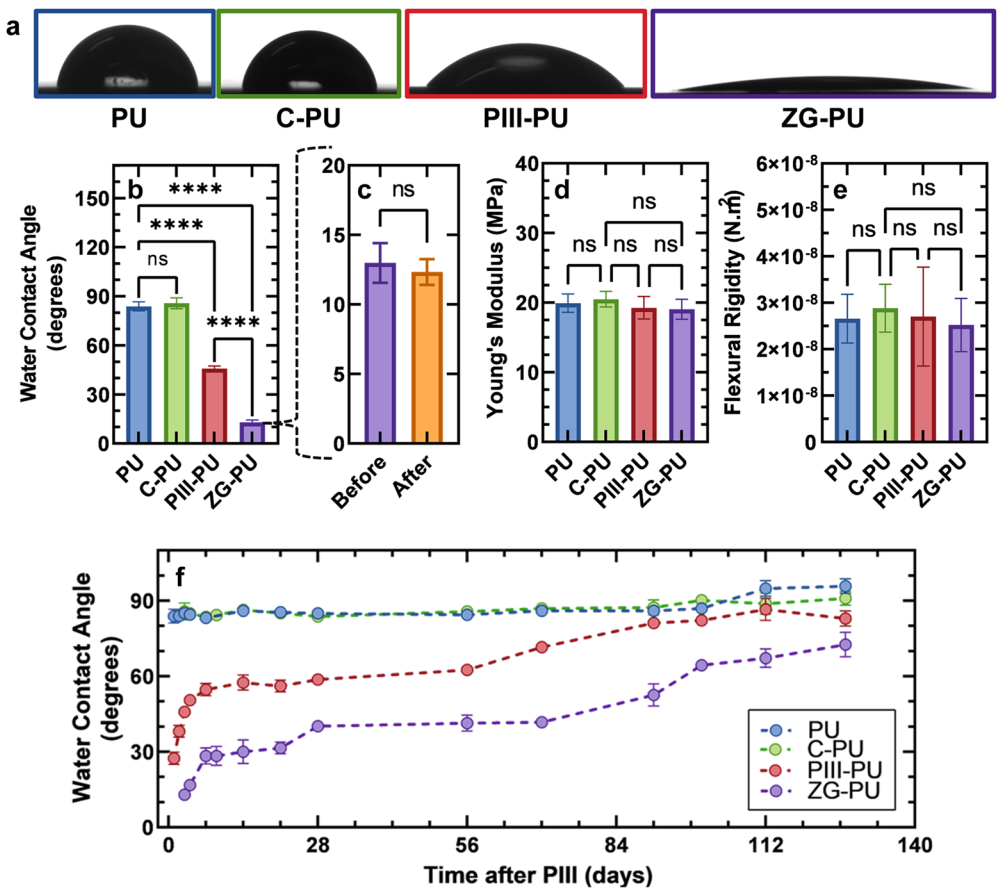

Fig. 3 | Surface and bulk polymer properties of ZG-PU. a Water contact angle was used to determine material hydrophilicity, with **b** ZG-PU being significantly more hydrophilic than controls, and **c** retained their hydrophilicity after an extensive mechanical bending programme comprising of 3000 bending cycles. The **d** Young's modulus and the **e** flexural rigidity of ZG-PU were not significantly different to the control samples. **f** Despite the success of the initial graft, ZG-PU (and PIII-PU) underwent substantial losses in hydrophilicity. Error bars are mean ± standard error; **** indicates a p-value < 0.0001.

polyzwitterion chains were either initiated and propagated in solution via free-radical polymerisation and then terminated via grafting to the substrate or initiated from the plasma-treated surface and propagated outwards into the solution. Removing the initiator from the grafting solution (i.e., initiator-free solution, Fig. 1a) may still allow the latter mechanism to occur due to the presence of surface-embedded radicals in the PIII-treated substrate; this concept is explored later in this study.

Hydrophobic recovery of ZG-PU

Despite the successful fabrication of zwitterion-grafted substrates, ZG-PU gradually lost its hydrophilicity over time, with the contact angle shifting from 12.98° to around 70° four months after fabrication (Fig. 3f). Similarly, PIII-PU samples became increasingly hydrophobic over the same time, almost returning to the hydrophobicity of the pristine PU material. There was a steep decrease in ZG-PU hydrophilicity during the first two weeks (1.55°/day increase in angle angle), followed by a shallower decrease thereafter (0.38°/day increase in angle angle). Throughout this period, ZG-PU remained more hydrophilic than PIII-PU, suggesting the continued presence of the zwitterion layer, albeit at diminishing concentrations. To explain this, the contribution of potential graft detachment was considered negligible due to its previously demonstrated resilience under mechanical deformation (Fig. 3c), and the similar trends in gradual increase of contact angle observed for PIII-PU (Fig. 3f) and other PIII-treated materials[54,55]. Instead, this observation may be due to hydrophobic recovery, wherein the mobile PU chains embed the polar zwitterionic motifs under the surface to minimise free energy at the air-surface interface (note that samples were stored exposed to air). A similar trend in hydrophobic recovery was observed when poly(methyl methacrylate) (PMMA) was successfully modified with plasma-induced zwitterion grafting using the same process to generate zwitterion-grafted PMMA (ZG-PMMA) (Supplementary Fig. 2a). The glass transition temperature for PMMA (~105 °C) is lower than the melting temperature of hard segments of PU (~160–180 °C), yet higher than the PU soft segments' glass transition temperature (<0 °C). suggesting that at room temperature PMMA chains are significantly less mobile than those of PU. While ZG-PMMA hydrophilicity decreased in the first few days, the subsequent plateau contrasted with the continued hydrophilic losses occurring in ZG-PU, with reduced PMMA chain mobility at room temperature limiting hydrophobic recovery phenomena in ZG-PMMA (Supplementary Fig. 2b). Notably, the rapid hydrophobic recovery in the days after PIII treatment (in the absence of zwitterion treatment) has been observed in highly mobile elastomers such as PU (Fig. 3 and Cheng et al.[54]), but also less mobile polymer chains such as PMMA (Supplementary Fig. 2) or polystyrene[55].

Importantly, the ultimate objective of zwitterionic modification assisted with PIII surface activation is to achieve long-term enhancement of substrate antifouling to extend the durability of devices in blood-contacting environments. As the antifouling functionality of zwitterions is rooted in their induced superhydrophilicity, the observed hydrophobic recovery would prove detrimental to device performance. Despite this, no long-term studies of zwitterion-grafted polymers have been reported beyond one month[27,35], with the limited literature offering contrasting findings. While a dopamine-mediated zwitterion-grafted poly(vinyl chloride) was reported to maintain its hydrophilicity after thirty days[35], another zwitterion-grafted PU fabricated via the Fenton reaction started to lose its hydrophilicity after seven days[27]. Moreover, there is little evidence regarding the maintenance of passive surface modifications such as zwitterions on PIII-functionalized substrates. To address this, further studies were conducted to subsequently optimise the fabrication process to minimise hydrophobic recovery.

Extending the lifetime of the zwitterionic grafted surfaces

Plasma treatment conditions. The impact of plasma functionalization on maintaining the effect of zwitterion grafting was studied by changing the PIII treatment time (i.e., the time of substrate exposure to plasma), the system voltage (i.e., changing the energy of the plasma particles) and the type of plasma functionalization. Accordingly, as PIII treatment time increased, the initial ZG-PU water contact angle slightly decreased, although this trend was only significant when comparing extremes (Fig. 4ai). Nonetheless, improvements in zwitterion grafting may be facilitated by increasing PIII time, agreeing with known correlations between treatment time, ion fluence, and free-radical concentration[55]; i.e., longer treatment times translate to increased ion fluence and free-radical concentration, thus augmenting interactions between the functionalized surface and zwitterions. However, changing treatment time had negligible effects on hydrophobic recovery (Fig. 4a-ii, 4a-iii and Supplementary Fig. 3a), indicating that treatment time could modulate the efficiency of zwitterion grafting, but not the propensity for hydrophobic recovery. Alternatively, the PIII voltage was decreased to reduce the penetration depth of the nitrogen ions. Lower voltages resulted in less hydrophilic ZG-PU surfaces, suggesting poorer zwitterion grafting (Fig. 4b-i), however, hydrophilic loss became notably flatter during the first two weeks (Fig. 4b-ii). At a voltage of 20 kV, the rate of hydrophilic loss in this period was 1.55°/day, while lower voltages of 15 kV and 10 kV correlated with flatter gradients of 0.99°/day and 0.87°/day, respectively. However, decreasing voltage likely reduced substrate functionalization, as implied by the higher initial water contact angles of PIII-PU materials fabricated with lower voltages (Supplementary Fig. 3b). Thus, lower voltage PIII may limit hydrophobic recovery but at the expense of grafting efficiency. In addition, a milder plasma treatment without ion implantation was also investigated with a plasma cleaner using compressed air under a slight vacuum (herein referred to as air plasma). This method also yielded ZG-PU, albeit with a slightly less hydrophilic surface than PIII-mediated ZG-PU (Fig. 4c–i and Supplementary Fig. 3c). The initial loss in hydrophilicity of air plasma-mediated ZG-PU was much steeper than PIII-mediated ZG-PU (Fig. 4c-ii), which can be attributed to the absence of a reservoir of embedded radicals. Without ion bombardment, air plasma treatment provides a shallow treatment depth (i.e., a few nanometres), whereas PIII can embed radicals in depth up to 100 nm under the surface[39]. After their initial rapid shifts, the longer-term hydrophobic recovery trends in both groups were the same (Fig. 4c-ii and Supplementary Fig. 3c). To this end, enhanced ion bombardment may benefit the zwitterionic graft via improved grafting and slight mitigation of short-term hydrophilic losses. These studies highlight the ability to optimise substrate functionalization (and thus the efficiency of the zwitterion grafting) via modifying plasma functionalization parameters. They simultaneously demonstrate the inability to maintain these properties by manipulating the plasma functionalization process itself.

Grafting time. Further studies focused on varying parameters in the zwitterion grafting step, namely zwitterion monomer concentration and the length of the grafting period (i.e., the time substrates were immersed in the zwitterion solution). Increasing zwitterion concentration trended towards improved hydrophilicity, until a threshold where hydrophilicity reduced (Supplementary Fig. 4a). The decreased hydrophilicity at the highest concentration (500 mg mL^{-1}) may be attributed to the sterically limited access of the polyzwitterion chains to the substrate surface; this agrees with previous literature that reports the necessity of carefully controlling the molecular density of surface modifications due to steric hinderances[56,57]. Beyond slight improvements in hydrophilicity, increasing the concentration did not change hydrophobic recovery, with all samples exhibiting similar trends over time (Supplementary Fig. 4b). Subsequently, the zwitterion grafting process was modified by altering the grafting period to increase the likelihood of zwitterionic interactions with the surface. Initially, ZG-PU was fabricated using a two-day grafting period; increasing this to five or seven days had a minimal effect on the resulting graft, as their hydrophilicity upon removal from solution was similar to their respective time points in ZG-PU with two-day grafting periods (Fig. 4d-i). However, extending the grafting period to fourteen days enhanced ZG-PU hydrophilicity when compared with the fourteen-day time point of ZG-PU with two-day grafting periods (Fig. 4d-i and Supplementary Fig. 5). Moreover, while ZG-PU with five- or seven-day

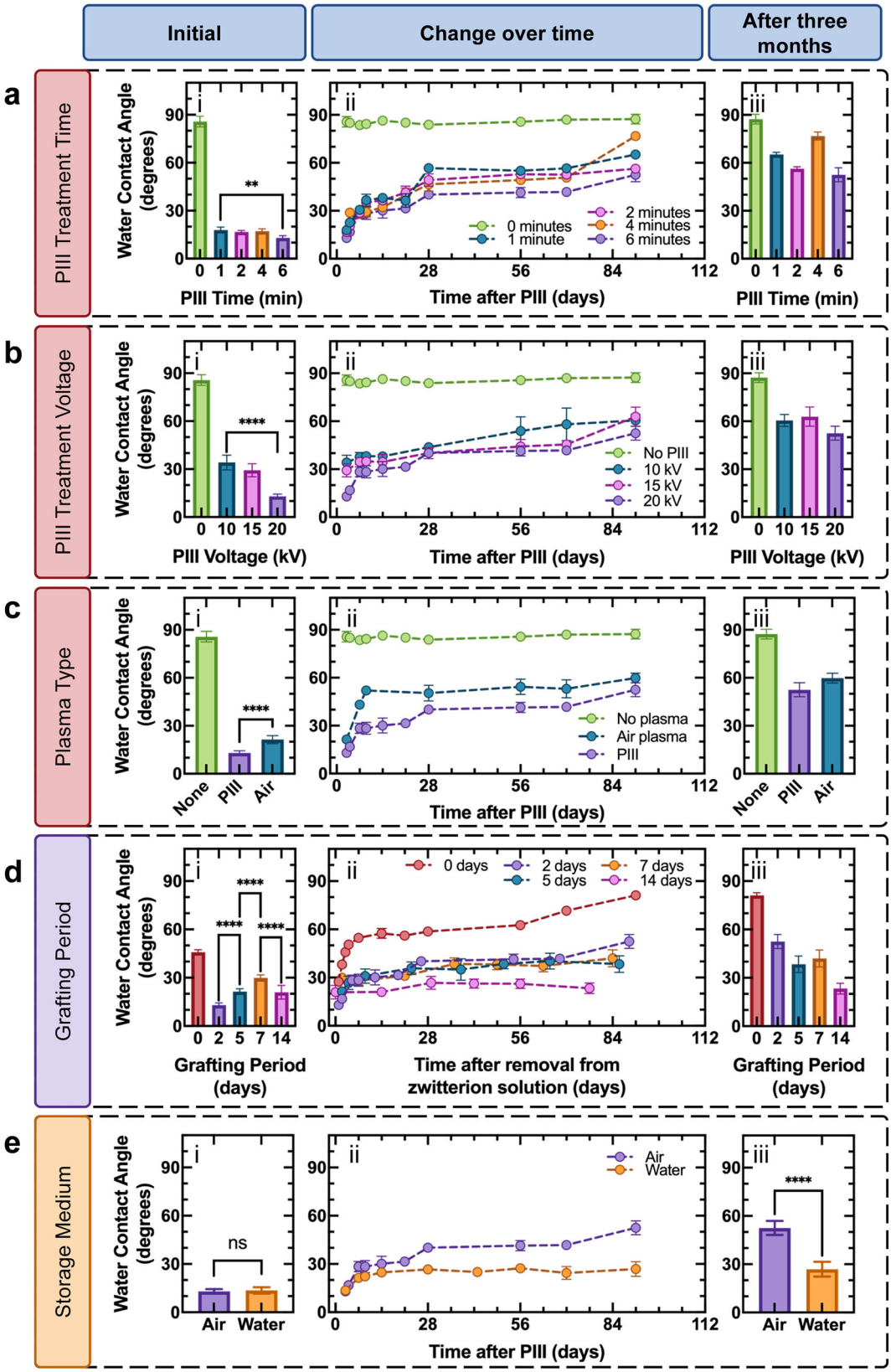

Fig. 4 | Optimisation studies aiming to maintain the zwitterionic surface chemistry, changing. a PIII treatment time, **b** PIII voltage, **c** plasma type, **d** length of the grafting period, and **e** storage of fabricated materials. Each study provides **(i)** the initial water contact angle, as a measure of hydrophilicity, after removal from solution (note that this is 48 h after PIII treatment for all studies except for D, where the grafting period is extended), **(ii)** the change in hydrophilicity over three months after fabrication, and **(iii)** the water contact angle at three months. Error bars are mean ± standard error; ** indicates a p-value < 0.01; **** indicates a p-value < 0.0001.

grafting periods followed similar hydrophobic recovery trends, a fourteen-day grafting period maintained its superhydrophilicity over three months (Fig. 4d-ii, d-iii), suggesting that extending the grafting period mitigates ZG-PU hydrophobic recovery. This observation may be ascribed to the reservoir of embedded radicals created by ion bombardment. Storing the PIII-treated substrate in the presence of zwitterion monomers over fourteen days enhances the grafting efficiency due to the continued interactions between the zwitterion moieties and radicals on the surface as embedded radicals migrate to the surface. The continuous reaction of zwitterion monomers with the surface-migrating radicals over a 14-day period seems to create a more stable zwitterion grafting layer which successfully mitigates the hydrophobic recovery.

Storage conditions. As hydrophobic recovery is hypothetically the outcome of polymer chains embedding polar elements to minimise interfacial free energy, it was theorised that maintaining a polar storage environment could also mitigate hydrophobic recovery. To this end, ZG-PU stored in water maintained a low water contact angle of ~25° up to three months after fabrication (despite only undergoing a two-day grafting period), indicating a substantially greater hydrophilic surface than ZG-PU stored in air (Fig. 4e). This observation further supports the hypothesis that hydrophilic recovery is governed mainly by localised arrangement of chains with respect to their environment. When stored in water, the free energy of the interface-media system is in its minimum state as long as the zwitterion-grafted moieties on the surface interact with the water molecules of the media. Exchanging water with air as the storage media, however, alters this thermodynamic balance, encouraging the surficial chains to rearrange locally and bury the more hydrophilic moieties inside. This process translates to an increase in water contact angle for samples stored in air. Recalling that the grafting time also led to maintaining a highly hydrophilic surface in samples with a fourteen-day grafting period even when stored in air after grafting (Fig. 4d), one can conclude that the grafting period leads to less mobile zwitterionic coating (e.g., larger grafted chains) that resists or delay the rearrangement of polymer chains in air.

Surface-initiated zwitterion grafting

A promising avenue for process optimisation also lay in the mechanism by which polyzwitterion chains were grafted to the polyurethane surface. Until this point, zwitterion was aided by a thermal radical initiator. This external initiator contributed to free-radical generation alongside the surface-embedded radicals that were created during the PIII process, allowing for grafting to occur through either termination or initiation events; that is, a combination of graft-to and graft-from mechanisms, respectively. Graft-to mechanisms involve the attachment of pre-formed or propagating polymer chains to the surface, whereas graft-from mechanisms involve surface-initiated polymerisation[58,59]. Both mechanisms are believed to occur during initiator-aided grafting (Fig. 5a). Subsequently, an initiator-free approach was explored to identify the utility of a truly graft-from mechanism as a means of both improving process scalability and maintaining the zwitterionic surface. To this end, PIII-functionalized PU substrates were immersed in a solution of zwitterion monomers without an external chemical initiator (Fig. 1a). The resulting ZG-PU demonstrated similar hydrophilicity (Fig. 5b) and wave-like morphologies to initiator-aided ZG-PU (Fig. 5c), and a sulphur-containing surface with a S/(C-C) ratio of 0.23 ± 0.01 (Fig. 5d, e), all confirming the successful initiator-free grafting of zwitterionic moieties.

Moreover, the initiator-free approach mitigated hydrophobic recovery when combined with a fourteen-day grafting period and a higher zwitterion monomer concentration (Fig. 5f and Supplementary Fig. 6). Previously, extending the grafting period conveniently addressed the sustained surface migration of embedded radicals (Fig. 3f). Removing the external initiator consequently allows this migration to offer a continuous supply of reactive sites for surface-initiated free-radical polymerisation, as well as sterically permitting the use of higher zwitterion concentrations by restricting surface interactions to monomer units rather than propagating polymer units. In fact, the surface architectures of an initiator-free approach are believed to be preferable to those of an initiator-aided approach, as the latter involves graft-to mechanisms. Graft-to approaches typically result in low-density grafts with non-ideal mushroom-like topologies, while graft-from approaches result in high-density grafts with ideal brush topologies[58,59] (Fig. 5a). At present, the exact architecture of the grafted polyzwitterions is not fully understood, although further work will elucidate these characteristics. Thus, an initiator-free strategy with longer grafting periods and higher zwitterionic concentrations substantially mitigated hydrophobic recovery in ZG-PU, indicating suitable processing parameters to maintain the zwitterionic surface. Furthermore, the lack of an external initiator and an initiating step minimises the reagents and infrastructure required for, and the waste produced by this process. Moreover, as the only solute in an initiator-free solution is zwitterion monomer, this may be reused to improve the throughput of the described process (Supplementary Fig. 7).

Preliminary antifouling and antithrombogenicity studies

Stable ZG-PU materials were fabricated by immersing PIII-functionalized PU in an initiator-free, high-concentration SBMA monomer solution for fourteen days, followed by storage in water. Preliminary biological tests were performed to evaluate the antifouling and anti-thrombogenic properties of ZG-PU five weeks after material fabrication. The antifouling performance of ZG-PU was evaluated via bovine serum albumin (BSA) and fibrinogen adsorption assays, and antithrombogenicity was evaluated via a static gravimetric coagulation assay. Firstly, BSA provides a useful model protein due to the abundance of (human) albumin among the proteins involved in biofouling[8]. PU adsorbed 1201 ± 429.98 μg cm^{-2} more albumin than the control, while ZG-PU adsorbed 1083 ± 210.12 μg cm^{-2} *less* than the control (Supplementary Fig. 8), indicating the antifouling properties of the zwitterion graft. Then, fibrinogen adsorption was assessed via a fluorescent assay wherein samples were immersed in fresh blood plasma enriched with fluorescently labelled fibrinogen (Fig. 6a). Fluorescent intensity on PU and ZG-PU was 2,564,505 ± 302,698 and 298,593 ± 32,167, respectively, which equated to ZG-PU fluorescence being approximately 11.6% of the fluorescence response of PU, suggesting that the zwitterion graft reduced fibrinogen adsorption by almost 9-fold. These studies importantly highlight the antifouling behaviour of ZG-PU in a general context (i.e., BSA), but also in the context of biofouling as a precursor for thrombosis (i.e., fibrinogen). Fibrinogen is one of the first proteins to adsorb onto foreign surfaces and is primarily responsible for platelet adhesion under low-shear conditions[8]. In the coagulation cascade, fibrinogen is converted to fibrin via thrombin and polymerises to form fibrous networks that stabilise blood clots[1,9]. Thus, the mitigation of fibrinogen adsorption offers a promising mechanism by which thrombosis may be similarly reduced.

To this end, material thrombogenicity was assessed via a gravimetric coagulation assay in heparinised whole blood (Fig. 6b). The thrombus mass on ZG-PU (0.70 ± 0.26 mg) was 26% of thrombus on pristine PU (2.65±0.18 mg), and even slightly lower than thrombus on expanded poly(tetrafluoroethylene) (ePTFE) (1.00±0.55 mg), an established and clinically used anti-thrombogenic material. These observations demonstrate the antithrombogenicity of ZG-PU, agreeing with myriad studies regarding the anti-thrombogenic behaviour of zwitterion modifications[24–26]. Additionally, thrombosis on ZG-PU was also lower than on a siloxane-based polyurethane (Si-PU) (2.00 ± 0.14 mg) (Fig. 6b). Importantly, Si-PUs were developed to address the thrombogenicity of other polyurethanes, although at the expense of bulk mechanics such as stiffness and toughness, whereas ZG-PU does not compromise the mechanics of the underlying PU (Fig. 3d, e). Moreover, non-optimised ZG-PU materials (i.e., ZG-PU materials developed in Section 2.1 prior to implementing the processes to maintain the zwitterionic surface chemistry) generated a thrombus mass of 2.63±0.23 mg, which was not significantly different to that of pristine PU (Fig. 6b). Both the optimised and non-optimised samples were tested five weeks after fabrication, at which point the sulphur content of the non-

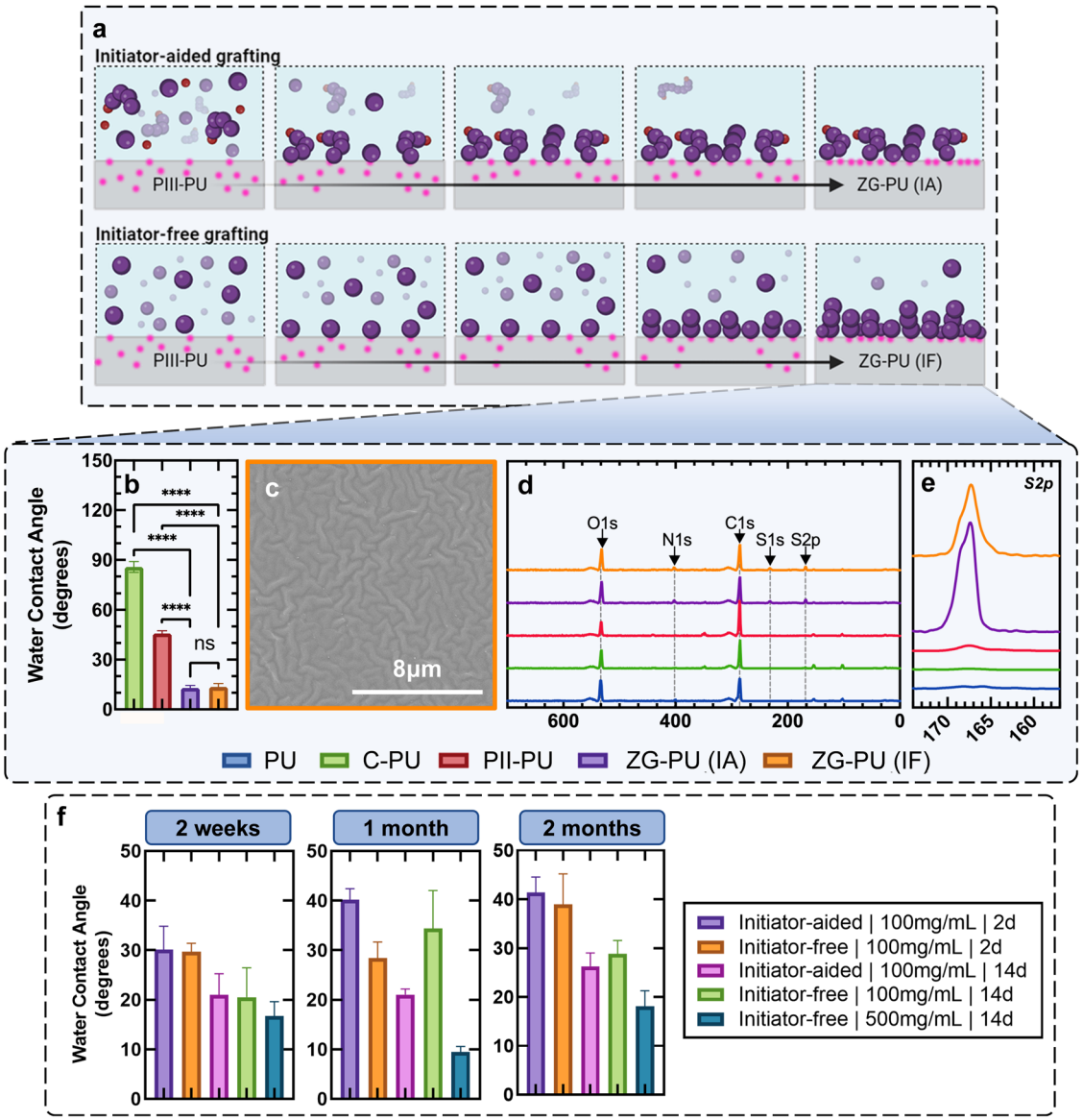

Fig. 5 | The effect of an initiator-free strategy on PIII-mediated zwitterion-grafted polyurethanes. a Initiator-aided strategies (upper row) involve a combination of (1) polymerisation of zwitterion chains in solution, followed by grafting to the functionalized surface (i.e., a graft-to mechanism), and (2) immobilisation of a zwitterion monomer by surface-embedded radicals on the functionalized substrate, initiating free-radical polymerisation from the surface (i.e., a graft-from mechanism). In comparison, initiator-free strategies (lower row) only exhibit the latter (graft-from) mechanism, allowing greater grafting densities than initiator-aided strategies due to sterically favourable interactions between the zwitterionic solute and the PIII-functionalized surface. Purple circles represent zwitterionic monomers, red circles represent initiator molecules, and pink circles represent surface-embedded radicals. Using an initiator-free approach, ZG-PU was successfully fabricated, demonstrating **b** similar hydrophilicity to initiator-aided ZG-PU (via water contact angle), **c** a distinctive wave-like morphology (via SEM), and **d**, **e** the emergence of sulphur peaks, indicating the presence of the sulfonate anion on the surface (via XPS); the x-axis units are binding energy (eV). **f** The long-term hydrophilicity of the fabricated ZG-PU was optimised when using an initiator-free strategy with a higher zwitterion monomer concentration and a fourteen-day grafting period. Note that these materials were stored in the air, allowing the improvements to be ascribed to the grafting strategy only. IF initiator-free, IA initiator-aided, 2d two-day grafting period, 14d fourteen-day grafting period. Error bars are mean ± standard error; **** indicates a p-value < 0.0001.

optimised ZG-PU material was approximately 30% that of the optimised ZG-PU material (Supplementary Fig. 9), suggesting a correlation between the removal of SBMA moieties from the surface and a reduction in anti-thrombogenic functionality. These findings underline the importance of the optimisation processes developed in this report as a crucial platform technology in ensuring the long-term antithrombogenicity of zwitterion-grafted materials. In other words, without careful analysis of the long-term maintenance of the surface chemistry, the proposed anti-thrombogenic behaviour of zwitterionic surface modifications will degrade over time. Importantly, more comprehensive in vitro and in vivo biological investigations will be required to further characterise the hemocompatibility of these materials, although these preliminary findings collectively demonstrate that the proposed surface modification technology facilitates chemically stable zwitterionic grafts that promise long-lasting antifouling and anti-thrombogenic properties.

Process versatility

Thus far, a carbonate-based polyurethane was used as a model substrate and a sulfonate-based zwitterion was used as a model zwitterion. However, this process is not restricted to this sole combination of components. In fact, this platform can be applied to a range of polymer substrates and zwitterion compounds. In addition to ZG-PMMA fabrication (Supplementary Fig. 2),

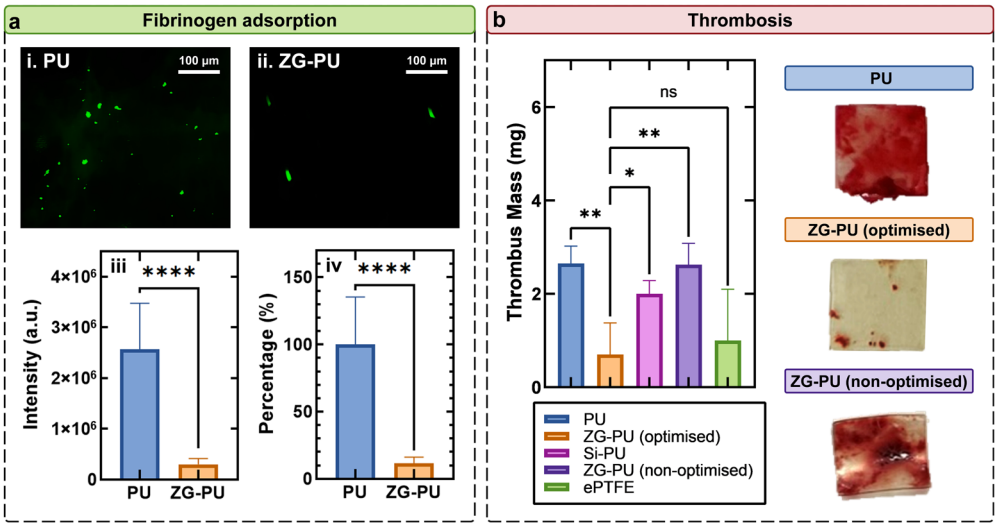

Fig. 6 | Evaluation of the antifouling and anti-thrombogenic properties of ZG-PU five weeks after material fabrication. a Fibrinogen adsorption on **(i)** PU and **(ii)** ZG-PU was assessed via a fluorescently labelled fibrinogen assay. **(iii, iv)** ZG-PU exhibited a fluorescence around 10% of the intensity of the PU fluorescence, indicating improved antifouling capabilities. **b** Thrombosis was assessed via a static gravimetric coagulation assay. Thrombus mass was measured for PU, ZG-PU, a siloxane-based polyurethane (Si-PU), a ZG-PU sample prepared without applying the processes developed to maintain surface chemistry, termed ZG-PU (non-optimised), and expanded poly(tetrafluoroethylene) (ePTFE), demonstrating lower coagulation on ZG-PU than PU, Si-PU, and ZG-PU (non-optimised), as well as similar behaviour to ePTFE, an established anti-thrombogenic material. Error bars are mean ± standard error; * indicates a p-value < 0.05; ** indicates a p-value < 0.01; **** indicates a p-value < 0.0001.

several other polymers were successfully modified, including poly(-caprolactone) (PCL, Fig. 7a), poly(vinyl chloride) (PVC, Fig. 7b), and poly(tetrafluoroethylene) (PTFE, Fig. 7c). For all systems the water contact angle decreased significantly (with respect to both the pristine material and its PIII-functionalized counterpart) and the surface composition shifted, collectively suggesting zwitterion grafting (Fig. 7, Supplementary Fig. 10 for full XPS survey). For this latter observation, all systems generated a sulphur (S2p) peak (Fig. 7a-iv, b-iv, c-iv) and a nitrogen (N1s) peak after grafting (Supplementary Fig. 10); just as sulphur is attributable to zwitterionic sulfonate anions, for these materials, nitrogen can be attributed to zwitterionic ammonium cations (Fig. 1a). Moreover, the surface coverage of these grafts can be observed in the XPS survey of ZG-PVC, wherein the chlorine peak (Cl2p) is significantly lower than for pristine PVC (Supplementary Fig. 10b), suggesting that the substrate surface is masked by a relatively dense zwitterion graft. To this end, this process would be applicable to a range of substrates that have well-established clinical and biological utility; for example, PVC is a common construction material for blood-contacting catheters[35] or blood bags[60], PTFE (in its expanded form) is used to fabricate vascular grafts and cardiovascular patches[61], and PCL offers a promising scaffold for tissue engineering in a range of systems (e.g., skeletal, cardiovascular, muscular, nervous) or as drug delivery devices[62].

Furthermore, an alternative zwitterion, 2-methacryloyloxyethyl phosphorylcholine (MPC) (Fig. 7d-i), was successfully grafted to PU, resulting in a similar hydrophilicity to SBMA-grafted ZG-PU (Fig. 7d-ii, d-iii, d-iv), and the development of a phosphorus peak in XPS analysis, which can be attributed to the zwitterionic phosphoryl group (Fig. 7d-v, d-vi). The ability to graft molecules to PIII-functionalized substrates via a carbon double bond has been reported elsewhere[63], indicating that a variety of methacrylated zwitterions may readily be grafted via this process, regardless of the exact structure of the zwitterionic side group. Recently, developments in zwitterionic molecular design have promised advances towards improved antifouling chemistries[64,65]. This suggests that employing the method proposed in this study can aid the grafting of a wide range of polymeric substrates with newer generations of zwitterionic modifications, provided a carbon double bond is included in the monomer structure. Taken together, these findings demonstrate the process developed in this report as a viable strategy for modifying various ready-made polymer-based medical devices with various commercial methacrylated zwitterions, potentially offering long-lasting antifouling properties in a range of blood-contacting applications.

Conclusion

The suboptimal performance of implanted polymeric materials due to their susceptibility to biofouling presents a significant challenge in the long-term clinical use of blood-contacting polymeric medical devices. In this report, an efficient and versatile process was proposed to improve the hemocompatibility of a wide range of polymeric substrates by grafting a durable polyzwitterionic layer via PIII functionalization of the underlying substrate. This polyzwitterionic layer transformed the surface of the hydrophobic substrates into near-superhydrophilic systems without compromising bulk mechanical properties. The fabrication process was optimised to maintain the superhydrophilic surface chemistry of the treated materials, which subsequently demonstrated antifouling and anti-thrombogenic behaviour in preliminary in vitro evaluations. Moreover, the optimised process negated the requirement for excessive wet chemistry reagents, chemical linkers, or chemical initiators, thus simultaneously streamlining the fabrication process and reducing chemical hazards and waste. This strategy demonstrates a pathway for enhancing the long-term biocompatibility of polymeric substrates via PIII functionalization of the substrate followed by surface-initiated free-radical zwitterionic polymerisation, providing a promising platform for the fabrication of durable blood-contacting devices.

Methods

Materials

A carbonate-based polyurethane (ChronoFlex C, Shore hardness 80A) and a siloxane-based polyurethane (ChronoSil, Shore hardness 80A) were purchased from AdvanSource Biomaterials. Tetrahydrofuran (THF), sulfobetaine methacrylate (SBMA), ammonium persulfate (APS), poly(caprolactone) (PCL, 80 kDa), poly(vinyl chloride) (PVC, high molecular weight), poly(methyl methacrylate) (PMMA, 120 kDa), and bovine serum albumin (BSA) were purchased from Sigma Aldrich.

Polyurethane film preparation

PU films were prepared by casting a 10 w/v% PU/THF solution in a glass Petri dish. These casts were evaporated for 24 h in a fume cupboard to produce PU films of approximately 150 μm thickness.

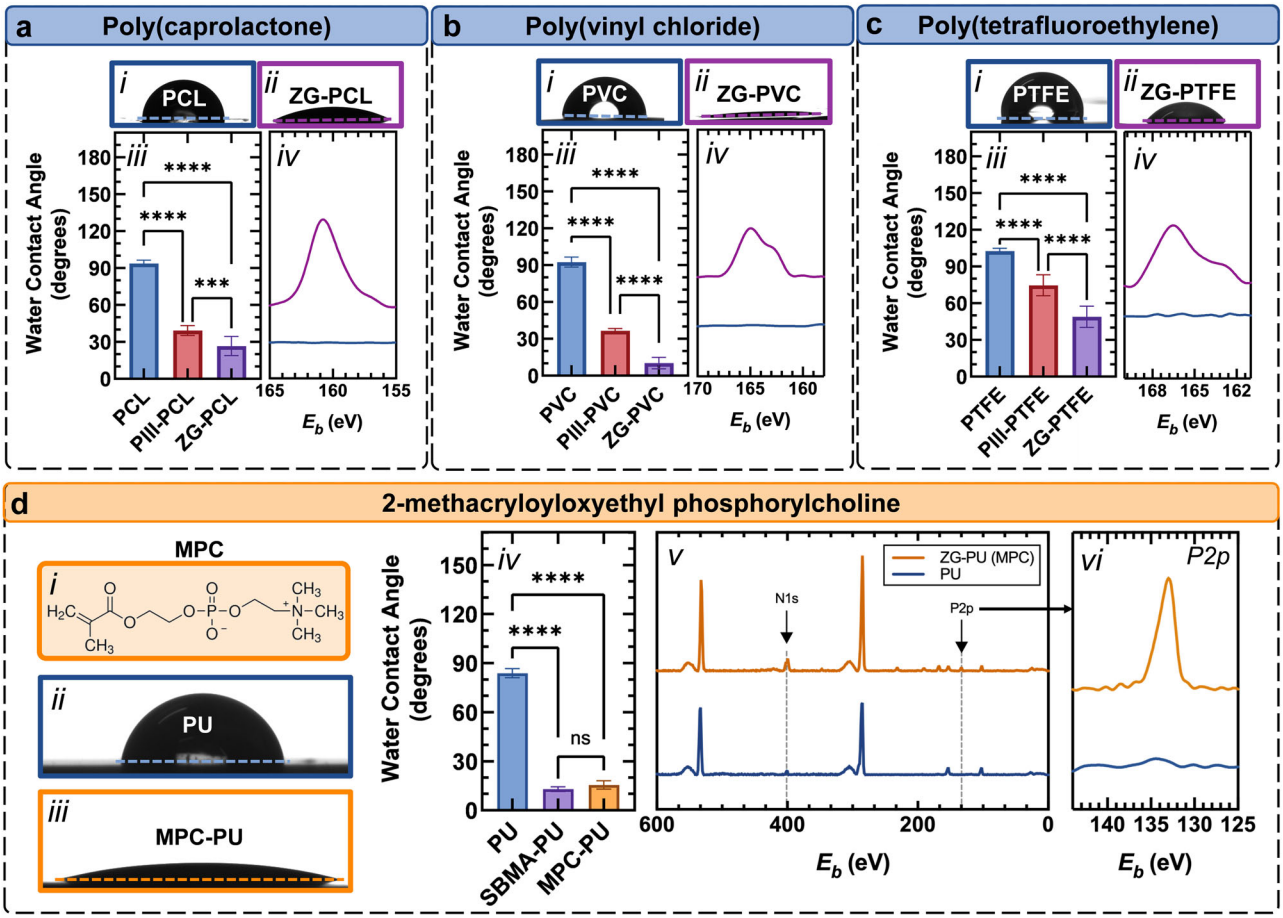

Fig. 7 | Process versatility was demonstrated by performing the process on different substrates. a PCL, **b** PVC, and **c** PTFE. For each material, the water contact angle of the **(i)** pristine material and the **(ii)** zwitterion-grafted material were **(iii)** significantly different, with **(iv)** the zwitterion-grafted materials (purple lines) possessing sulphur as identified by XPS analysis of the S2p spectrum. (**d**) A different zwitterionic monomer **(i)** (2-methacryloyloxyethyl phosphorylcholine) was successfully grafted to **(ii)** PU, resulting in **(iii)** an MPC-grafted ZG-PU (MPC-PU) that **(iv)** was much more hydrophilic than PU and similar to SBMA-grated ZG-PU (SBMA-PU), and **(v)** possessed phosphorus as identified by XPS analysis of the P2p spectrum. Note that SBMA-PU is the same as ZG-PU described throughout this report and is renamed here to avoid confusion in comparison with MPC-PU. Error bars are mean ± standard error; *** indicates a p-value < 0.001; **** indicates a p-value < 0.0001.

Zwitterion solution preparation

Initiator-aided zwitterion solutions. SBMA was dissolved in MQ water at a concentration of 100 mg mL^{-1}. APS was then added at a concentration of 0.1 mol% based on the stoichiometry of SBMA in the solution. A stir bar was placed in the solution, and the solution was placed into an ice bath on top of a stir plate to facilitate solution mixing while maintaining a cold environment. At the same time, the solution was degassed by bubbling nitrogen through the solution for 30 min. Different concentrations of SBMA solution were made via the same method.

Initiator-free zwitterion solutions. These solutions were made in a similar manner to the initiator-aided solutions but without the addition of APS.

PIII treatment

PIII treatment was carried out using a custom-made system, previously described in detail[66]. 6 × 5 cm PU films were attached to the sample holder and a mesh was fixed over the sample surface. This holder system was mounted into the PIII chamber and electrically connected to the high-voltage PIII unit. The chamber was vacuumed to at least 2×10^{-5} Torr, before supplying nitrogen gas to the chamber, bringing the chamber pressure to 2×10^{-3} Torr. Nitrogen plasma was generated via a radiofrequency power of 100 W, which was then accelerated towards the PU substrate via 20 kV pulses, each of 20 µs and with a frequency of 50 Hz. PIII treatment was conducted for 360 s, unless otherwise stated. During process optimisation, the pulsed high voltages of 15 kV and 10 kV, and PIII treatment times of 300, 240, 180, 120 and 60 s were used. After treatment, the materials were carefully removed from the PIII system and placed in polystyrene dishes for zwitterion grafting.

Zwitterion grafting

Initiator-aided approach. Plasma-functionalized PU films were fixed to the bottom of polystyrene dishes in a zwitterion solution prepared for the initiator-aided process. The dishes were sealed with paraffin and aluminium foil and placed in the oven at 60 °C for 48 h, unless otherwise stated. After this time, the samples were removed from the solution and washed thoroughly at least three times with MQ water. The films were carefully cleaned with a lint-free wipe to remove the macroscopic polymer synthesised in solution. The materials were then immersed in MQ water for at least 6 h before washing three times with water. For initiator-aided samples that extended polymerisation time, the samples remained in solution for their respective time periods, however, were still removed from heat after 48 h.

Initiator-free approach. Plasma-functionalized PU films were placed in polystyrene dishes in a zwitterion solution prepared for the initiator-free process. These dishes were sealed with paraffin and stored at room temperature for 48 h. Then, the samples were removed from the solution and washed thoroughly at least three times with water. Although no macroscopic polymer was formed in the solution, the surface was still carefully cleaned with a lint-free wipe. The materials were then immersed

in MQ water for at least 6 h before washing three times with water. For initiator-free samples that extended polymerisation time, the samples were simply kept in solution for that length of time before undergoing the described washing procedure.

Conventional air plasma treatment

Conventional air plasma treatment was performed using a plasma cleaner (PDC-002-HP Plasma Cleaner, Harrick Plasma) under a slight vacuum (200 Torr) with a compressed air feed. PU samples were fixed inside the treatment chamber, the chamber was vacuumed and then plasma treatment was performed for 360 s. After plasma treatment, materials were grafted with zwitterions via identical protocols used for PIII-treated materials.

Material characterisation

Surface imaging. The materials were imaged using scanning electron microscopy (Phenom™ XL G2 Desktop SEM, Thermo Fisher Scientific) operating with a backscatter electron detector with a 15 kV acceleration voltage. Before loading into the microscope, materials were sputter coated with a 16 nm thick gold/palladium layer via a plasma sputter coater. Materials were also imaged using Atomic Force Microscopy (NeaSNOM, Neaspec), with images processed using Gwyddion software. For both methods, at least 4 samples were imaged, with the most representative image displayed.

Water contact angle. Material hydrophilicity was analysed by measuring the water contact angle of the surface ($n = 6$) using a static sessile drop method at room temperature (DSA25B Drop Shape Analyser, KRÜSS). 5 µL droplets were dispensed at a rate of 200 µL min^{-1} and carefully touched to the surface of the loaded material to transfer from the syringe to the material. The droplet on the material surface was imaged 10 s after deposition using a high-resolution IEEE 1394 camera, and the water contact angle was measured using the instrument software.

Elemental analysis. The surface chemistry of the samples ($n = 3$) was analysed using X-ray Photoelectron Spectroscopy (K-alpha$^+$ XPS, Thermo Fisher Scientific). Samples were mounted onto a standard sample stage and then loaded into the XPS machine. The XPS experiment was constructed using the connected software (Avantage Data System, Thermo Fisher Scientific). The X-ray gun spot size was set to 400 µm, and the flood gun was turned on. For each material, XPS survey, C1s, O1s, N1s and S2p spectra were obtained (ten times each). As sulphur-containing compounds may be damaged by X-ray radiation, the S2p spectra were obtained first, followed by the XPS survey, C1s, O1s, and N1s spectra. The resulting data was analysed using the Avantage software.

Tensile properties. The tensile properties of the materials were characterised by a tensile test using a mechanical testing machine (Instron BioPuls 5943). Samples were cut into 30 × 5 mm strips ($n = 8$) and loaded into the machine to allow a material length of 20 mm in between the clamps. A tensile test method was run with a strain rate of 50 mm min^{-1}. Force (F) and displacement (Δl) were converted to tensile stress (σ) and tensile strain (ε) by normalising by the samples' cross-sectional area and initial length, respectively. Young's modulus (E) was calculated as the gradient in the elastic region of the resulting stress-strain graphs.

$$\sigma = \frac{F}{A_c}$$

$$\varepsilon = \frac{\Delta l}{l_i}$$

$$E = \frac{\sigma}{\varepsilon}$$

Flexural properties. The flexural properties of the materials were calculated using a uniformly loaded cantilever beam test, allowing the calculation of the flexural rigidity via a derivation of the Euler-Beam theory. Samples were prepared into strips ($n = 8$) that allowed a 15 mm length (L) of material for testing, plus enough to anchor the sample at one end. Sample mass was measured, and the uniform load on the strip (q) was calculated by dividing sample mass by testing length. The strips were anchored at one end and allowed to flex under the uniform load of gravity. The flexed samples were imaged, and the angle of deflection (ϕ) calculated manually. Flexural rigidity (EI) was then calculated using the following equation:

$$EI = \frac{qL^3}{6\phi}$$

Cyclic bending. 50 × 40 mm ZG-PU materials were prepared using an initiator-aided strategy and the hydrophilicity determined using a water contact angle, as previously described. Samples were then subject to a cyclic bending protocol under hydrated conditions to determine the effect of mechanical manipulation on graft attachment. Samples were loaded into a mechanical testing machine (Instron BioPlus), allowing for 30 mm of material in between the clamps. The entire sample and clamp system were then immersed in a water bath. A cyclic compression method with a strain rate of 15 mm.min^{-1} and a compression displacement of 20 mm was performed for 3000 cycles. The compression method allowed for the sample (a film) to bend upon machine compression. After completion of the method, samples were removed from the water bath, air dried for 2 h and then the water contact angle measured again.

Antifouling and hemocompatibility

BSA adsorption. Bovine serum albumin adsorption was evaluated via a fluorescent assay. Six 1cm^2 squares of PU and ZG-PU materials were fixed in the wells of a BSA-blocked 24-well plate. 1 mL of a 40 mg mL^{-1} solution of BSA in PBS was added for 18 h, after which point 150 µL of the BSA solution from each well was pipetted into a fluorescence-specific 96-well plate. 50 µL of fluorescamine was pipetted into each well plate and the plate was immediately loaded into a fluorescent spectrometer and scanned between 400 and 500 nm wavelengths. The resulting absorbance (A) was correlated to a BSA concentration (C_{BSA}) via a pre-determined calibration curve:

$$A = \left(870.07 \times C_{BSA}\right) + 15,759$$

The difference between this concentration and the initial concentration was used to determine the mass of BSA absent from the solution (based on the initial volume used), with this quantity assuming to have adsorbed to the material or the fluorescent well plate. To correct for this latter occurrence, six samples of a 40 mg mL^{-1} BSA solution without any material immersion were prepared in the initial 24-well plate, and then fluorescence was measured similarly to the test samples. The difference between the initial concentration and the concentration of the control solution was assumed to be due to adsorption to either the initial well plate or the fluorescent well plate and was then subtracted from the test results. The remaining difference was used to calculate the BSA mass adsorbed to the immersed materials, resulting in an estimation of BSA adsorption density.

Fibrinogen adsorption. 1 cm^2 films of each sample (PU, ZG-PU) were prepared and attached to the bottom of a BSA-coated 24-well plate. Whole blood was withdrawn under sterile conditions, combined with 3×10^{-4} v/v% heparin, and centrifuged at 1000 rpm for 15 min. Plasma was collected and combined 1:1 with a fibrinogen working solution containing AlexaFluor 488 conjugated fibrinogen from human plasma at a concentration of 40 µg mL^{-1} in PBS. The combined serum-fibrinogen solution was placed on ice and 750 µL was pipetted into each well. Samples were incubated at 37 °C while agitated at 65 rpm for 40 min. Each sample was removed from the well plate and carefully washed in PBS solution. Samples were imaged using a Zeiss Z1 Inverted fluorescent

microscope, and the intensity of the resulting images was calculated using Image J software.

Thrombosis. 1 cm^2 films of each sample (PU, ZG-PU, ZG-PU-unstable, ePTFE, PCL) were prepared, weighed, and attached to the bottom of a BSA-coated 24-well plate. Whole blood was withdrawn under sterile conditions and combined with 3×10^{-4} v/v% heparin. The heparinised whole blood was immediately placed on ice and 750 µL was pipetted into each well. The plate was incubated at 37 °C while agitated at 65 rpm for 40 min. Each material was then removed from the well plate and carefully washed in PBS solution. Samples were left to air dry and then weighed again. The difference in mass between the measurements before and after exposure to blood was calculated as the mass of the thrombus adhered to the material.

Process versatility

The same PIII modification and initiator-free zwitterion grafting steps were performed on PMMA, PTFE, PCL and PVC materials using the same parameters as described above. Similarly, PU samples were functionalized via identical PIII treatment protocols but then grafted with 2-methacryloyloxyethyl phosphorylcholine (MPC) instead of sulfobetaine methacrylate, however using the same parameters as described above. Characterisation via water contact angle and XPS was also performed similarly. For XPS, specific spectra were analysed for each material; fluorine for PTFE, chlorine for PVC, and phosphorus for MPC-grafted PU.

Statistical analysis

DATA. Statistical significance involving multiple comparisons was assessed using one-way ANOVA with Tukey correction. Statistical significance between the two datasets was assessed using an unpaired, two-tailed *t*-test. For water contact angle data, measurements for any given time were taken from distinct samples, although these samples were then measured repeatedly over different time points. For all other data, measurements were always taken from distinct samples. Data is presented as mean ± standard error, with *p*-values denoted as follows: $^{*}p < 0.05$, $^{**}p < 0.01$, $^{***}p < 0.001$, $^{****}p < 0.000$.

Reporting summary

Further information on research design is available in the Nature Portfolio Reporting Summary linked to this article.

Data availability

The data supporting this scientific work are available from the corresponding author upon reasonable request.

Received: 29 September 2023; Accepted: 21 February 2024;
Published online: 05 March 2024

References

1. Jaffer, I. H. & Weitz, J. I. The blood compatibility challenge. Part 1: Blood-contacting medical devices: The scope of the problem. *Acta Biomater.* **94**, 2–10 (2019).
2. Crago, M., Winlaw, D. S., Farajikhah, S., Dehghani, F. & Naficy, S. Pediatric pulmonary valve replacements: Clinical challenges and emerging technologies. *Bioeng. Transl. Med.* e10501, https://doi.org/10.1002/btm2.10501. (2023).
3. Citla Sridhar, D., Abou-Ismail, M. Y. & Ahuja, S. P. Central venous catheter-related thrombosis in children and adults. *Thromb. Res.* **187**, 103–112 (2020).
4. Talebian, S. et al. Biopolymeric coatings for local release of therapeutics from biomedical implants. *Adv. Sci.* **10**, 2207603 (2023).
5. Baumann Kreuziger, L., Jaffray, J. & Carrier, M. Epidemiology, diagnosis, prevention and treatment of catheter-related thrombosis in children and adults. *Thromb. Res.* **157**, 64–71 (2017).
6. MacIsaac, S. et al. How did we get here?: a historical review and critical analysis of anticoagulation therapy following mechanical valve replacement. *Circulation* **140**, 1933–1942 (2019).
7. Crago, M. et al. The evolution of polyurethane heart valve replacements: How chemistry translates to the clinic. *Mater. Today Commun.* **33**, 104916 (2022).
8. Brash, J. L., Horbett, T. A., Latour, R. A. & Tengvall, P. The blood compatibility challenge. Part 2: Protein adsorption phenomena governing blood reactivity. *Acta Biomater.* **94**, 11–24 (2019).
9. Alkarithi, G., Duval, C., Shi, Y., Macrae, F. L. & Ariëns, R. A. S. Thrombus structural composition in cardiovascular disease. *Arterioscler. Thromb. Vasc. Biol.* **41**, 2370–2383 (2021).
10. Maan, A. M. C., Hofman, A. H., de Vos, W. M. & Kamperman, M. Recent developments and practical feasibility of polymer-based antifouling coatings. *Adv. Funct. Mater.* **30**, 2000936 (2020).
11. Gunatillake, P. A. et al. Advancements in the development of biostable polyurethanes. *Polym. Rev.* **59**, 391–417 (2019).
12. Maitz, M. F. et al. The blood compatibility challenge. Part 4: Surface modification for hemocompatible materials: Passive and active approaches to guide blood-material interactions. *Acta Biomater.* **94**, 33–43 (2019).
13. Biran, R. & Pond, D. Heparin coatings for improving blood compatibility of medical devices. *Adv. Drug Deliv. Rev.* **112**, 12–23 (2017).
14. Schlenoff, J. B. Zwitteration: coating surfaces with zwitterionic functionality to reduce nonspecific adsorption. *Langmuir* **30**, 9625–9636 (2014).
15. Stallard, C. P., McDonnell, K. A., Onayemi, O. D., O'Gara, J. P. & Dowling, D. P. Evaluation of protein adsorption on atmospheric plasma deposited coatings exhibiting superhydrophilic to superhydrophobic properties. *Biointerphases* **7**, https://doi.org/10.1007/s13758-012-0031-0. (2012).
16. Sivaraman, B. & Latour, R. A. The relationship between platelet adhesion on surfaces and the structure versus the amount of adsorbed fibrinogen. *Biomaterials* **31**, 832–839 (2010).
17. Leslie, D. C. et al. A bioinspired omniphobic surface coating on medical devices prevents thrombosis and biofouling. *Nat. Biotechnol.* **32**, 1134–1140 (2014).
18. Lowe, S., O'Brien-Simpson, N. M. & Connal, L. A. Antibiofouling polymer interfaces: poly(ethylene glycol) and other promising candidates. *Polym. Chem.* **6**, 198–212 (2014).
19. Erathodiyil, N., Chan, H.-M., Wu, H. & Ying, J. Y. Zwitterionic polymers and hydrogels for antibiofouling applications in implantable devices. *Mater. Today* **38**, 84–98 (2020).
20. Sin, M.-C., Chen, S.-H. & Chang, Y. Hemocompatibility of zwitterionic interfaces and membranes. *Polym. J.* **46**, 436–443 (2014).
21. Blackman, L. D., Gunatillake, P. A., Cass, P. & Locock, K. E. S. An introduction to zwitterionic polymer behavior and applications in solution and at surfaces. *Chem. Soc. Rev.* **48**, 757–770 (2019).
22. Shao, Q., He, Y., White, A. D. & Jiang, S. Difference in hydration between carboxybetaine and sulfobetaine. *J. Phys.Chem. B* **114**, 16625–16631 (2010).
23. Bretscher, M. S. & Raff, M. C. Mammalian plasma membranes. *Nature* **258**, 43–49 (1975).
24. McVerry, B. et al. A readily scalable, clinically demonstrated, antibiofouling zwitterionic surface treatment for implantable medical devices. *Adv. Mater.* 2200254, https://doi.org/10.1002/adma.202200254. (2022).
25. Smith, Roger et al. Vascular catheters with a nonleaching poly-sulfobetaine surface modification reduce thrombus formation and microbial attachment. *Sci. Transl. Med.* **4**, 153ra132–153ra132 (2012).

26. Ukita, R. et al. Zwitterionic poly-carboxybetaine coating reduces artificial lung thrombosis in sheep and rabbits. *Acta Biomater.* **92**, 71–81 (2019).
27. Lee, S. Y., Lee, Y., Le Thi, P., Oh, D. H. & Park, K. D. Sulfobetaine methacrylate hydrogel-coated anti-fouling surfaces for implantable biomedical devices. *Biomater. Res.* **22**, 3 (2018).
28. Dong, D. et al. High-strength and fibrous capsule–resistant zwitterionic elastomers. *Sci. Adv.* **7**, eabc5442 (2021).
29. Liu, K. et al. Chemical bonding of biological valve leaflets with an aminated zwitterionic copolymer for long-term anticoagulation and improved anti-calcification. *Chem. Eng. J.* **426**, https://doi.org/10.1016/j.cej.2021.131803. (2021).
30. Guo, F. et al. Artificial heart valves with balanced charged networks exhibiting anti-calcification properties. *ACS Appl. Bio Mater.* **3**, 838–847 (2020).
31. Huang, Z., Nazifi, S., Cheng, K., Karim, A. & Ghasemi, H. Scalable inter-diffused zwitterionic polyurethanes for durable antibacterial coatings. *Chem. Eng. J.* **422**, 130085 (2021).
32. Zhang, Z. et al. Blood compatibility of surfaces with superlow protein adsorption. *Biomaterials* **29**, 4285–4291 (2008).
33. Zhang, L. et al. Zwitterionic hydrogels implanted in mice resist the foreign-body reaction. *Nat. Biotechnol.* **31**, 553–556 (2013).
34. Lin, X. et al. Photoreactive carboxybetaine copolymers impart biocompatibility and inhibit plasticizer leaching on polyvinyl chloride. *ACS Appl. Mater. Interfaces* **12**, 41026–41037 (2020).
35. Liu, Y. et al. A uniform and robust bioinspired zwitterion coating for use in Blood-contacting catheters with improved anti-inflammatory and antithrombotic properties. *Macromol. Biosci.* **21**, https://doi.org/10.1002/mabi.202100341. (2021).
36. Asha, A. B., Chen, Y. & Narain, R. Bioinspired dopamine and zwitterionic polymers for non-fouling surface engineering. *Chem. Soc. Rev.* **50**, 11668–11683 (2021).
37. Golabchi, A., Wu, B., Cao, B., Bettinger, C. J. & Cui, X. T. Zwitterionic polymer/polydopamine coating reduce acute inflammatory tissue responses to neural implants. *Biomaterials* **225**, 119519 (2019).
38. Qiao, Y. et al. Dopamine-mediated zwitterionic polyelectrolyte-coated polypropylene hernia mesh with synergistic anti-inflammation effects. *Langmuir* **36**, 5251–5261 (2020).
39. Zhianmanesh, M., Gilmour, A., Bilek, M. M. M. & Akhavan, B. Plasma surface functionalization: A comprehensive review of advances in the quest for bioinstructive materials and interfaces. *Appl. Phys. Rev.***10**, https://doi.org/10.1063/5.0130829. (2023).
40. Chang, Y., Chang, W.-J., Shih, Y.-J., Wei, T.-C. & Hsiue, G.-H. Zwitterionic sulfobetaine-grafted poly(vinylidene fluoride) membrane with highly effective blood compatibility via atmospheric plasma-induced surface copolymerization. *ACS Appl. Mater. Interfaces* **3**, 1228–1237 (2011).
41. Venault, A. et al. Antifouling pseudo-zwitterionic poly(vinylidene fluoride) membranes with efficient mixed-charge surface grafting via glow dielectric barrier discharge plasma-induced copolymerization. *J. Membr. Sci.* **516**, 13–25 (2016).
42. Akamatsu, K., Noto, W., Fukuzawa, H., Hara, A. & Nakao, S.-I. Grafting of carboxybetaine polymers to polyethylene membranes via plasma graft polymerization to improve low-fouling properties and to tune the molecular weight cut-off. *Sep. Purif. Technol.* **204**, 298–303 (2018).
43. Burmeister, N. et al. Surface grafted N-oxides have low-fouling and antibacterial properties. *Adv. Mater. Interfaces* 2300505, https://doi.org/10.1002/admi.202300505. (2023).
44. Burmeister, N. et al. Zwitterionic surface modification of polyethylene via atmospheric plasma-induced polymerization of (vinylbenzyl-) sulfobetaine and evaluation of antifouling properties. *Colloids Surf B: Biointerfaces* **224**, 113195 (2023).
45. Bilek, M. M. M. et al. Free radical functionalization of surfaces to prevent adverse responses to biomedical devices. *Proc. Natl Acad. Sci. USA* **108**, 14405–14410 (2011).
46. Liu, Q. et al. Zwitterionically modified alginates mitigate cellular overgrowth for cell encapsulation. *Nat. Commun.* **10**, https://doi.org/10.1038/s41467-019-13238-7. (2019).
47. González-Henríquez, C. M. et al. Innovative procedure for precise deposition of wrinkled hydrogel films using direct inkjet printing. *Mater Design* **194**, 108959 (2020).
48. Balcerowski, T., Ozbek, B., Akbulut, O. & Dumanli, A. G. Hierarchical organization of structurally colored cholesteric phases of cellulose via 3D printing. *Small* **19**, 2205506 (2023).
49. Wang, S., Liu, K., Yao, X. & Jiang, L. Bioinspired surfaces with superwettability: new insight on theory, design, and applications. *Chem. Rev.* **115**, 8230–8293 (2015).
50. Kondyurina, I. et al. Plasma mediated protein immobilisation enhances the vascular compatibility of polyurethane with tissue matched mechanical properties. *Biomed. Mater. (Bristol)* **12**, 045002–045002 (2017).
51. Ruhoff, A. M. et al. Biomaterial wettability affects fibrin clot structure and fibrinolysis. *Adv. Healthcare Mater.* **10**, 2100988 (2021).
52. Wakelin, E. A., Davies, M. J., Bilek, M. M. M. & McKenzie, D. R. Temperature activated diffusion of radicals through ion implanted polymers. *ACS Appl. Mater. Interfaces* **7**, 26340–26345 (2015).
53. Kosobrodova, E. A. et al. Free radical kinetics in a plasma immersion ion implanted polystyrene: theory and experiment. *Nucl. Instrum. Method. Phy. Res. Sect. B: Beam Interact. Mater. Atom.* **280**, 26–35 (2012).
54. Cheng, X., Kondyurin, A., Bao, S., Bilek, M. M. M. & Ye, L. Plasma immersion ion implantation of polyurethane shape memory polymer: surface properties and protein immobilization. *Appl. Surf. Sci.* **416**, 686–695 (2017).
55. Kosobrodova, E., Kondyurin, A., McKenzie, D. R. & Bilek, M. M. M. Kinetics of post-treatment structural transformations of nitrogen plasma ion immersion implanted polystyrene. *Nucl. Instrum. Methods Phys. Res. Sect. B: Beam Interact. Mater. Atom.* **304**, 57–66 (2013).
56. Chang, Y., Chen, S., Zhang, Z. & Jiang, S. Highly protein-resistant coatings from well-defined diblock copolymers containing sulfobetaines. *Langmuir* **22**, 2222–2226 (2006).
57. Uchida, K., Otsuka, H., Kaneko, M., Kataoka, K. & Nagasaki, Y. A reactive poly(ethylene glycol) layer to achieve specific surface plasmon resonance sensing with a high S/N ratio: the substantial role of a short underbrushed PEG layer in minimizing nonspecific adsorption. *Analyt. Chem.* **77**, 1075–1080 (2005).
58. Murad Bhayo, A., Yang, Y. & He, X. Polymer brushes: synthesis, characterization, properties and applications. *Prog. Mater. Sci.* **130**, 101000 (2022).
59. Yan, J., Bockstaller, M. R. & Matyjaszewski, K. Brush-modified materials: control of molecular architecture, assembly behavior, properties and applications. *Prog. Polym. Sci.* **100**, 101180 (2020).
60. Lin, X. et al. Zwitterionic carboxybetaine polymers extend the shelf-life of human platelets. *Acta Biomater.* **109**, 51–60 (2020).
61. Roina, Y., Auber, F., Hocquet, D. & Herlem, G. ePTFE functionalization for medical applications. *Mater. Today Chem.* **20**, 100412 (2021).
62. Mondal, D., Griffith, M. & Venkatraman, S. S. Polycaprolactone-based biomaterials for tissue engineering and drug delivery: current scenario and challenges. *Int. Journal of Polym. Mater. Polym. Biomater.* **65**, 255–265 (2016).
63. Walia, R. et al. Hydrogel−solid hybrid materials for biomedical applications enabled by surface-embedded radicals. *Adv. Funct. Mater.* **30**, 2004599 (2020).
64. Shao, Q. & Jiang, S. Molecular understanding and design of zwitterionic materials. *Adv. Mater.* **27**, 15–26 (2015).
65. Li, B. et al. Trimethylamine N-oxide–derived zwitterionic polymers: a new class of ultralow fouling bioinspired materials. *Sci. Adv.* **5**, eaaw9562 (2019).
66. Kondyurin, A. et al. Plasma ion implantation of silk biomaterials enabling direct covalent immobilization of bioactive agents for enhanced cellular responses. *ACS Appl. Mater. Interfaces* **10**, 17605–17616 (2018).

Acknowledgements
The authors acknowledge the financial support of the Australian Research Council (DP200102164), Medical Research Future Fund (MRFF, ARGCHD000015), and NSW Health (CVD Collaborative Grant 2022). The authors acknowledge Bingyan Liu for providing training on the use of the PIII instrument. The authors acknowledge Sydney Analytical for providing access and training for chemical analytical instruments, particularly Michelle Woods for atomic force microscopy, and Ahmed Ahmed for X-ray photoelectron spectroscopy. The authors also acknowledge the facilities in the Engineering Analytical Facility at The University of Sydney.

Author contributions
Matthew Crago: conceptualisation, methodology, investigation, formal analysis, validation, writing—original draft, writing—review & editing, visualisation. Richard Tan: methodology (thrombosis, fibrinogen adsorption), writing—review & editing. Juichien Hung: methodology (thrombosis, fibrinogen adsorption), writing—review & editing. Steven G. Wise: resources, writing—review & editing. Behnam Akhavan: methodology (PIII treatment), resources, writing—review & editing. Marcela Bilek: methodology (PIII treatment), resources. Fariba Dehghana: resources, writing—review & editing Sepehr Talebian: methodology (BSA adsorption), supervision, writing—review & editing. Sina Naficy: conceptualisation, methodology, resources, supervision, project administration, funding acquisition, writing—review & editing.

Competing interests
MC and SN declare that the concepts outlined in this manuscript are the subject of an Australian Provisional Patent Application (No. 2023903076). All other authors declare no competing interests.

Additional information
Supplementary information The online version contains supplementary material available at https://doi.org/10.1038/s43246-024-00462-y.

Correspondence and requests for materials should be addressed to Sina Naficy.

Peer review information *Communications Materials* thanks the anonymous reviewers for their contribution to the peer review of this work. Primary handling editors: Vishal Govind Rao and Jet-Sing Lee. A peer review file is available.